ISBN: 978-3-95450-224-0 ISSN: 2673-7035 doi:10.18429/JACoW-FLS2023-TU4P17

NON-DESTRUCTIVE VERTICAL HALO-MONITORS ON THE ESRF ELECTRON BEAM

K. Scheidt
European Synchrotron Radiation Facility, Grenoble, France

Abstract

The ESRF EBS storage ring has now among its electron beam diagnostics two independent units of vertical Halo-monitor. They use the available X-rays in a non-used Front-End, emitted from standard 0.56 T dipole magnets in the EBS lattice. These instruments measure continuously at a 2 Hz rate the so-called 'far-away' halo level, i.e. in a zone of roughly 1-3 mm away from the beam centre.

Both units are yielding excellent and well-correlated results with data of both the beam lifetime and of our 128 Beam Loss Detectors, and this as a function of the beam current, the filling-patterns, the vertical emittance, and the quality and incidents of the vacuum.

NON-DESTRUCTIVE MEASUREMENTS OF THE VERTICAL BEAM HALO

The Extreme Brilliant Source (EBS) ring at the European Synchrotron Radiation Facility (ESRF) is operational since mid-2020, generating coherent and bright X-rays for the scientific users. The X-rays are generated by an electron beam of 6 GeV and 200 mA, with horizontal and vertical emittances of 120 pm and 10 pm. A large range of diagnostics are in operation since the commissioning to measure the parameters, characteristics and behaviour of the beam [1, 2]. This 10 pm emittance implies that the beam's vertical size is in a range of roughly 4.5 to 13 um σ.

However, it is easily verified that a non-negligible beam population exists at some millimetres vertical distance from the beam-centre by inserting a vertical scraper and measuring the signal from a down-stream Beam Loss Detector (BLD). However, such method is destructive to the beam and not useable for assessing the halo population while serving normal users' operation (USM).

In 2014, in the old ESRF ring, a non-destructive vertical Halo-monitor based on imaging the X-rays from an available bending magnet beam-port was conceived and installed [3]. It was successfully operated and yielded excellent results until the disassembly of that ring for the subsequent installation of the new low emittance lattice of EBS in 2019. However, implementing a similar Halo-monitor in EBS was more complicated due to the constraints of the much smaller vacuum chamber, the weaker field strength of the available magnet source (now 0.56 T while 0.86 T before) and the longer distances between the essential components (now 6.8 m while before 4.2 m). These disadvantages were partly compensated by the availability of now non-used bending magnet Front-Ends, and this allowed a low-cost installation in cells 10 and 11 of two identical devices without any modification to the vacuum chambers in the EBS.

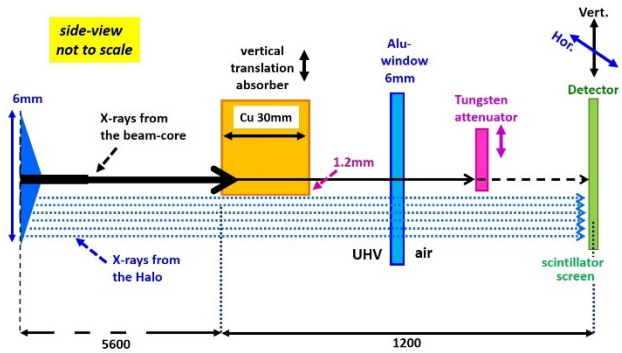

Figure 1: The main components and the paths of the X-rays of both the beam-core and that of the halo population.

Explanation of the Concept and its Components

The main components are shown in Fig. 1 in the vertical plane together with the (simplified) trajectory of the X-rays that are emitted from the electrons (at extreme left of the picture) and travel towards the detector (extreme right) which is a two-dimensional X-ray imager read-out by a standard camera. It is important to note that the X-rays from the central beam-core are many orders of magnitude stronger than those emitted from the electrons that make up the weak halo population. The specificity in our concept is to attenuate this powerful X-ray beam by an absorber that is vertically positioned so to intercept that beam.

However, the X-rays of typically 60 keV have a small but not a zero divergence as is supposed in the illustration. In fact, this divergence amplitude is 1E-9 for a divergence angle of 200 μrad. Therefore, the absorber (at roughly 6m from the source) needs to positioned at least 1.2 mm below the central axis, so to reduce this unwanted divergence signal to a negligible level compared to the weak level of the X-rays emitted by the halo. Consequently, it implies that this system can only detect the halo levels at roughly 1 to 3 mm distance from the beam-core.

The UHV of the Front-End is separated from the free air by a 6 mm thick Aluminium window. Further downstream a movable attenuator (1 mm thick Tungsten) provides flexibility in attenuation, followed by the detector that can be precisely positioned with a two-axis translation stage.

This detector is protected by a 5 mm thick lead box, and contains a 2 mm thick LYSO scintillator (15 x 15 mm), a double chicane with 3 mirrors, a set of achromat lenses and a CMOS camera and covers an 8 x 6 mm field of view.

The Fig. 2 shows a typical image (left) and its vertical profile (right). The beam-core signal there is produced by the main beam with its X-rays very strongly attenuated by the 30mm Copper, the 6 mm Aluminium and the 1 mm Tungsten. While for the halo signal beneath, the X-rays are only attenuated by the 6 mm Aluminium window. In the

ISBN: 978-3-95450-224-0 ISSN: 2673-7035 doi:10.18429/JACoW-FLS2023-TU4P17

commission period of this device, the edges of the Copper and Tungsten absorbers were optimized vertically, so to satisfy two conditions: a) let the X-rays emitted from the halo signal avoid these absorbers and b) intercept the divergent X-rays emitted from the main central beam so to ensure that these do not create a fake (background) signal in that lower zone where the system is supposed to only measure the genuine halo level. However, it implies a 'blind zone' where the system cannot measure.

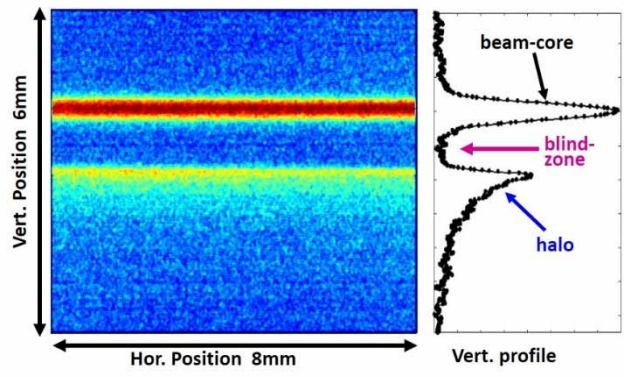

Figure 2: The typical image obtained shows clearly the beam core and the halo (below).

It is important to verify that this signal that we attribute to be the halo is not polluted by some parasitic signal by scattered X-rays, or from an incorrect positioning of the vertical absorber. In our storage ring we can use the vertical scraper to do such verification by positioning this scraper edge very close w.r.t. to the electron beam. By doing this in a relative fast scan, during which the scraper is typically put at distances of 3 to 0.3 mm in steps of 0.1 mm, and by measuring the halo levels at each step with a 1sec measurement time, we observe the progressive reduction and the final extinction of the halo level in our Halo-monitor.

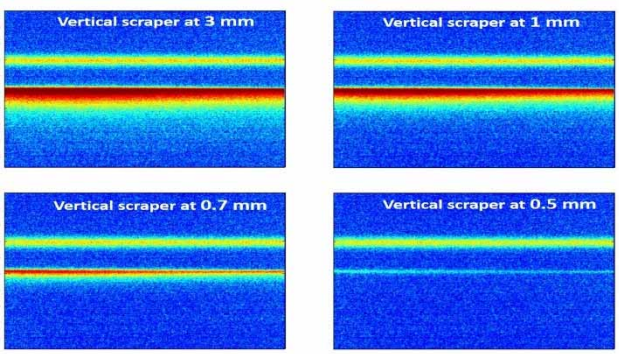

Figure 3: Verification results using the vertical scraper to check that halo signal is not polluted by a parasitic signal.

RESULTS UNDER NUMEROUS BEAM CONDITIONS AND MANIPULATIONS

These two new Halo-monitors are a useful addition to our existing scope of diagnostics systems, and their results can be directly compared with that of a) the lifetime monitor and b) the sum of all our 128 individual electron beam loss detectors. The latter we call "Losses" hereafter.

Figure 4 shows the curves of the rough data of lifetime (top), losses (middle) and the halo-levels (bottom) as a function of the beam current, up to 200 mA, with a uniform fill and a vertical emittance at 10 pm. It is emphasized that both the losses and the halo-levels are always expressed in arbitrary units.

In fact, in contrast to the beam lifetime measurement yielding an absolute and calibrated value, the BLD system, by definition, only measures a fraction of the (real total electron) losses, and the Halo-monitors only a fraction of the vertical halo-strength. However, it is now possible to normalize the results of both these losses and these halo-levels against that of the beam current and the inverse of beam lifetime. The result of this normalisation is shown in Fig. 5 over this same current range of 20 to 200 mA.

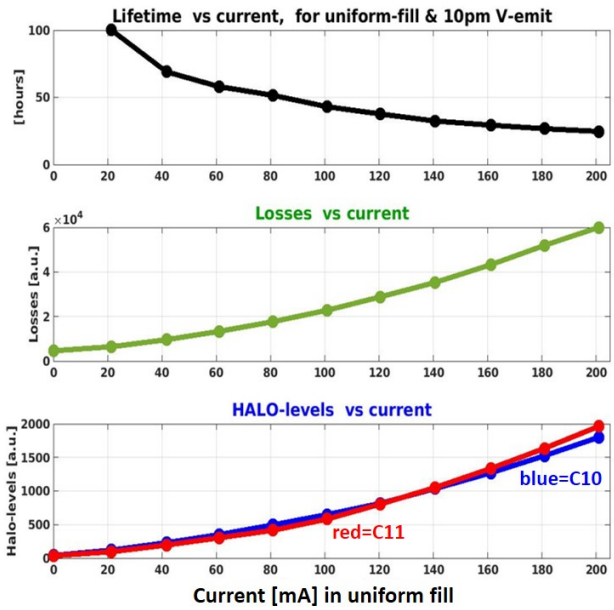

Figure 4: The signals of the beam lifetime, beam-losses, and the 2 Halo-monitors versus beam current.

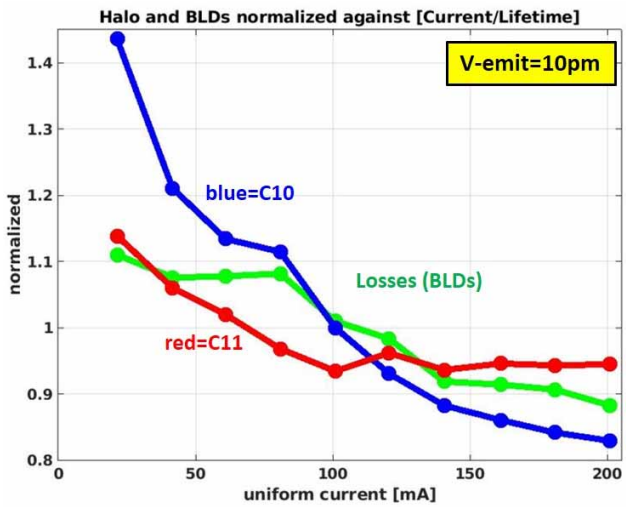

Figure 5: The normalized signals of the two Halo-monitors and of the beam-losses, versus beam current.

ISBN: 978-3-95450-224-0 ISSN: 2673-7035 doi:10.18429/JACoW-FLS2023-TU4P17

If all was perfect or ideal then these curves in Fig. 5 would be flat at value 1. The discrepancy is noticeable, and not further discussed or explained here, but of a reasonable low extent of about ± 10%.

Another set of data is shown in Fig. 6 in which the same values of lifetime, losses and halo-levels were recorded but this time for a stable beam current (74 mA in 16 bunch filling) while varying the vertical emittance between 1 and 50 pm. A system of adding a controlled vertical beam excitation is typically used for obtaining any wanted vertical emittance.

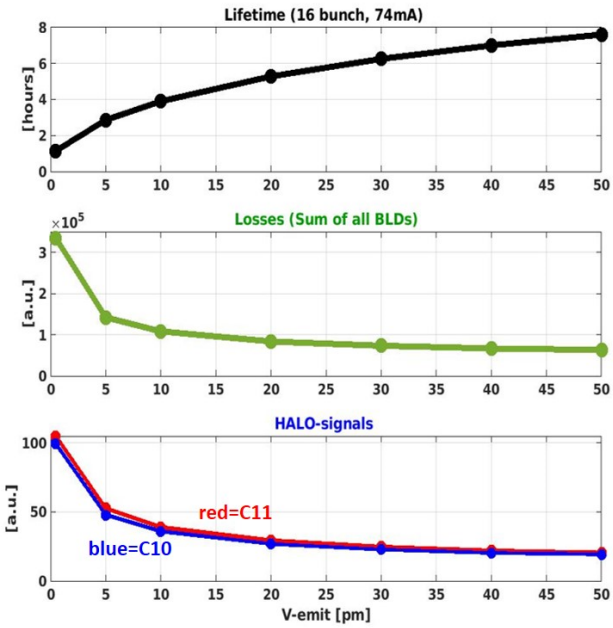

Figure 6: The signals of the beam lifetime, beam-losses, and the 2 Halo-monitors versus vertical emittance.

The same normalization is performed on this data and shown in Fig. 7 and an even better agreement (i.e. low discrepancy of ±10%) can be noted.

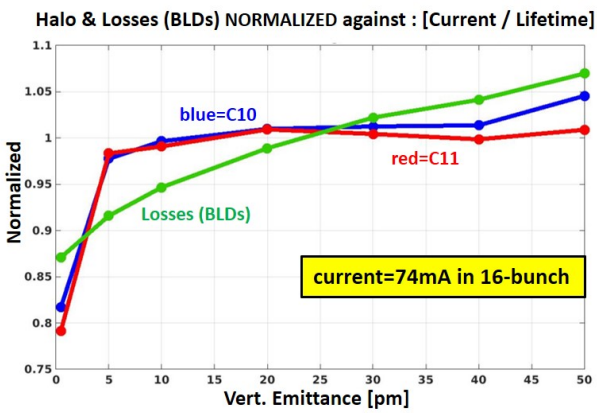

Figure 7: The normalized signals of the two Halo-monitors and of the beam-losses, versus vertical emittance.

A 3rd study was done in which the beam current in 16 bunch filling was varied up to 75 mA range, and this for a vertical emittance of 10 and 20 pm. The Fig. 8 shows the raw data while the Fig. 9 the normalized results of the BLD system and of the average of the two Halo-monitors. The Halo-monitor here shows a marked jump at 40-50 mA which is not yet explained, and needs to be re-measured and verified later.

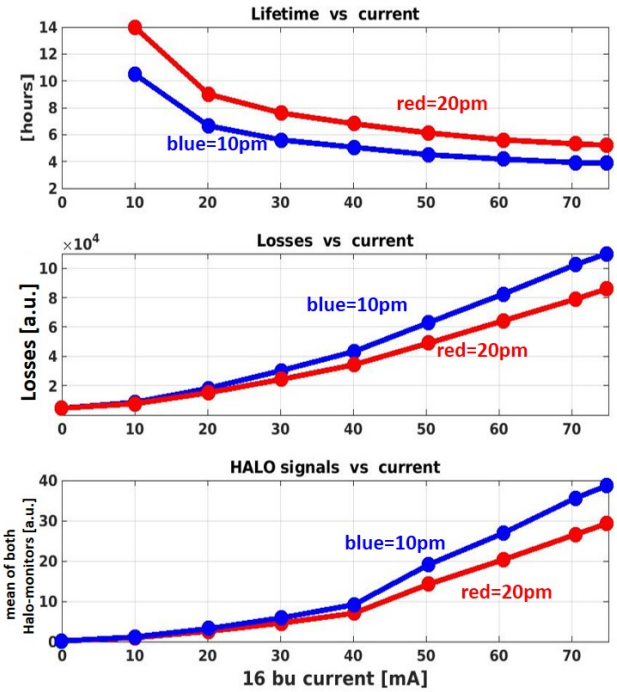

Figure 8: The signals of beam lifetime, beam-losses, and (mean of the) Halo-monitors versus beam current in 16-bunch fill, for values of 10 and 20 pm vertical emittance.

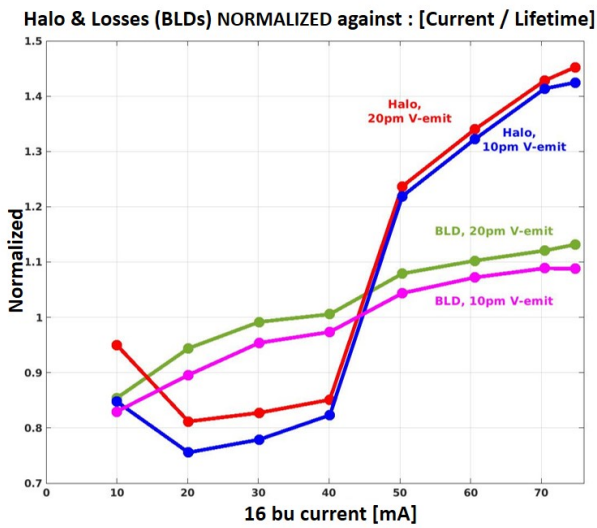

Figure 9: The normalized signals of the Halo-monitor and of the beam-losses, versus beam current, for 10 and 20 pm.

HALO SIGNALS DURING USM

The Halo-monitors provide data at 2 Hz which is stored in the database at the same rate. The same database also holds data of the beam current, beam lifetime, loss-levels of each of the 128 BLDs and the UHV pressure values of several hundreds of vacuum gauges.

ISBN: 978-3-95450-224-0 ISSN: 2673-7035 doi:10.18429/JACoW-FLS2023-TU4P17

The Fig. 10 shows a short -5% drop of the lifetime (from 5.25 to 5.0 hrs) and a +9% increase of the Losses while the Halo-monitors show both about 200% increase with much details, and an excellent signal-to-noise ratio and a quasi-perfect coherence between the two units.

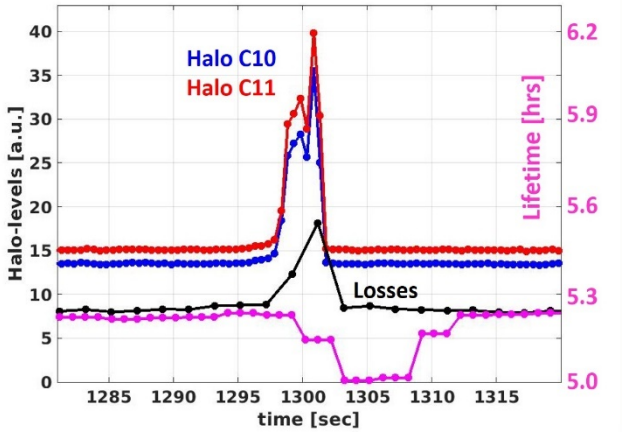

Figure 10: typical results during USM from the two Halo-monitors, the BLDs and the beam lifetime at the moment of a tiny fractional beam loss (16 bunch July 2023)

Such electron beam loss events occur rather frequently, but with very strongly varying levels, i.e. many events of the order of 1E-4 - 1E-6, while much rarer cases of >1E-3. In such latter case all related diagnostics detect and measure such event, and also the readings of the vacuum gauges can be correlated with it.

Smaller losses (e.g. 1E-4) are still easily detected by the BLDs but often not seen by the vacuum gauges, and barely detectable by the current monitor or the lifetime measurement. The two independent Halo-monitors have an extreme sensitivity to these very weak (but numerous) events. As such they constitute an 'watch-dog' to the slightest incident on the UHV vacuum quality.

The effect of, and the correlation with, the vacuum quality was assessed very neatly by creating temporarily an impaired local vacuum by switching on one of the titanium sublimators in the ring. The Fig. 11 shows the result of this manipulation.

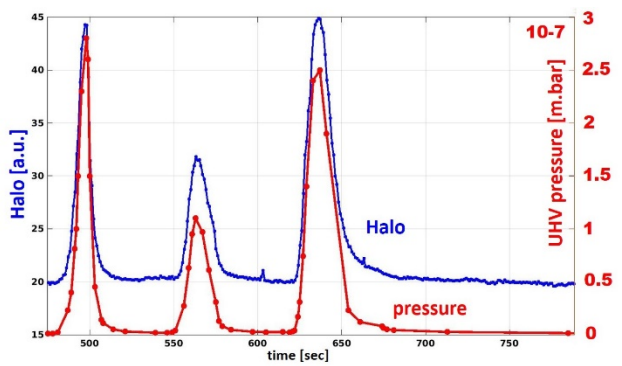

Figure 11: The excellent correlation between the halo level and the vacuum pressure on three specific events.

CONCLUSION AND PROSPECTS

The non-destructive Halo-monitor is a novice, reliable and sensitive diagnostic yielding direct information on the strength of the 'far-away' halo population of the ESRF's electron beam in its vertical plane. During USM this halo level shows to be extremely sensitive to the slightest change of beam parameters and notably to the incidence of small perturbations to the vacuum quality.

Certain accelerator studies have recently started to asses these halo levels as a function of the beam's coupling resonance, the beam's chromaticity, the minimum gap settings of our numerous in-vacuum insertion devices and the settings of our horizontal collimators. These studies will be pursued in the near future to further exploit this diagnostic.

ACKNOWLEDGMENTS

The author would like to thank the Front-End group for the support during the installation, the colleagues in the Beam Dynamics group for helpful discussions, and the ACU unit for the development of the software applications. Strong thanks are expressed to Diagnostics group colleagues Nicolas Benoist and Elena Buratin for the work of preparation, assembly and verification of these instruments.

REFERENCES

[1] L. Torino *et al.*, "Overview on the diagnostics for EBS-ESRF", in *Proc. IBIC'19*, Malmö, Sweden, Sep. 2019, pp. 9-13. doi:10.18429/JACoW-IBIC2019-MOA003

[2] L. Torino *et al.*, "Beam instrumentation performances through the ESRF-EBS commissioning", in *Proc. IBIC'20*, Santos, Brazil, Sep. 2020, pp. 11-16. doi:10.18429/JACoW-IBIC2020-MOA004

[3] K. B. Scheidt, "Non-destructive vertical Halo monitor on the ESRF's 6GeV electron beam", in *Proc. IBIC'14*, Monterey, CA, USA, Sep. 2014, paper MOCYB1, pp. 2-6

[4] E. Buratin and K. B. Scheidt, "New X-rays diagnostics at ESRF: The X-BPMs and the Halo-Monitor", in *Proc. IBIC'22*, Kraków, Poland, Sep. 2022, pp. 125-128. doi:10.18429/JACoW-IBIC2022-MOP34

[5] B. K. Scheidt, "The non-destructive vertical Halo monitor on the ESRF electron beam", presented at DEELS'22, HZB Berlin, Germany, June 2022, https://events.hifis.net/event/358/contributions/2263/